Equivalence of Effective Non-Hermitian Hamiltonians in the Context of Open Quantum Systems and Strongly Correlated Electron Systems

Yoshihiro Michishita* and Robert Peters†
Department of Physics, Kyoto University, Kyoto 606-8502, Japan

(Received 5 February 2020; accepted 20 April 2020; published 11 May 2020)

Recently, it has become clear that non-Hermitian phenomena can be observed not only in open quantum systems experiencing gain and loss but also in equilibrium single-particle properties of strongly correlated systems. However, the circumstances and requirements for the emergence of non-Hermitian phenomena in each field are entirely different. While the implementation of postselection is a significant obstacle to observe the dynamics governed by a non-Hermitian Hamiltonian in open quantum systems, it is unnecessary in strongly correlated systems. Until now, a relation between both descriptions of non-Hermitian phenomena has not been revealed. In this Letter, we close this gap and demonstrate that the non-Hermitian Hamiltonians emerging in both fields are identical, and we clarify the conditions for the emergence of a non-Hermitian Hamiltonian in strongly correlated materials. Using this knowledge, we propose a method to analyze non-Hermitian properties without the necessity of postselection by studying specific response functions of open quantum systems and strongly correlated systems.

DOI: 10.1103/PhysRevLett.124.196401

Introduction.—Recently, phenomena described by an effective non-Hermitian Hamiltonian (NHH) are intensively studied, especially in the context of open quantum systems (OQS) [1–12]. Effective NHH can induce novel topological phases [1,11,13–17] and unique phenomena such as anomalous edge states [7,14], skin effects [18–24], unusual quantum critical phenomena [8,12,25], unidirectional invisibility [26–28], chiral transport [6,29–32], and enhanced sensitivity [9,33–38]. Although the total Hamiltonian is Hermitian, the dynamics of the partial system alone can be described by an effective NHH, if the observed particle number of the partial system does not change during the time evolution. An unchanged particle number in the partial system can be achieved by applying postselection. However, postselection becomes exceedingly difficult because the probability of finding a system with an unchanged particle number decreases exponentially [39]. Thus, the study of non-Hermitian phenomena in OQS has been limited to small systems.

Besides experimental and theoretical studies of effective NHH in the context of OQS, Kozii and Fu [42] demonstrated that an effective NHH describes the single-particle properties in strongly correlated systems (SCS), which can result in the emergence of exceptional points and Fermi arcs in the spectral function. The spectral function or other response functions can be calculated by the single-particle Green's function, $G^R(\omega,\boldsymbol{k}) = [\omega - \mathcal{H}_0(\boldsymbol{k}) - \Sigma(\omega,\boldsymbol{k})]^{-1}$, where H_0 is the noninteracting part of the Hamiltonian and $\Sigma(\omega,\boldsymbol{k})$ is the self-energy. The self-energy is represented by a non-Hermitian matrix describing the correlations between particles, where the imaginary part of the self-energy describes the decay of a single-particle excitation. The single-particle Green's function can thus be written as $G^R(\omega,\boldsymbol{k}) = [\omega - \mathcal{H}_{\mathrm{eff}}(\omega,\boldsymbol{k})]^{-1}$, where $\mathcal{H}_{\mathrm{eff}}(\omega,\boldsymbol{k}) = \mathcal{H}_0(\boldsymbol{k}) + \Sigma(\omega,\boldsymbol{k})$ is an effective NHH. It has been shown that non-Hermitian properties of the effective Hamiltonian are related to correlation effects [40,43–48] and might be used to explain controversially discussed phenomena, such as quantum oscillations in topological Kondo insulators [49] or the pseudogap phase in high-Tc cuprates [42]. It is interesting to note that in the context of Green's functions in SCS, postselection, which is usually difficult to realize, is not necessary to detect non-Hermitian phenomena.

Until now, studies of effective NHH in the context of OQS and SCS are proceeding nearly independently from each other. It is unclear whether a relation between the effective NHH in both fields exists, and why postselection is not necessary in the context of SCS, while it is a big obstacle in experimental studies of non-Hermitian phenomena in OQS.

In this Letter, we demonstrate that the NHH describing the Green's function is equal to the NHH describing a single particle coupled to the rest of particles acting as a bath under postselection. For this purpose, we analyze the dynamics of a single particle in the Hubbard model using the quantum master equation (QME) in the context of OQS. The equivalence of the NHH in the single-particle spectral function and in the QME makes it possible to study non-Hermitian phenomena in OQS by analyzing certain response functions without applied postselection. Our analysis furthermore reveals why postselection is not

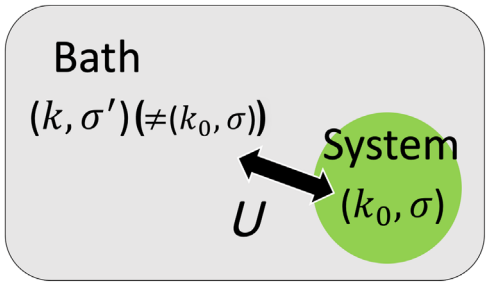

FIG. 1. To derive an effective non-Hermitian Hamiltonian for the single-particle dynamics in the Hubbard model in the context of OQS, we divide the electrons into a system, including only one particle, and the rest of the particles, acting as bath.

necessary to observe non-Hermitian phenomena in the context of single-particle Green's functions.

Quantum master equation for the Hubbard model.— First, we derive the QME for the dynamics of a single particle in a strongly correlated material. Furthermore, we demonstrate that the effective NHH in the context of OQS under postselection corresponds to that in the single-particle Green's function in the context of SCS. We here use the Hubbard model as a prototypical model describing SCS. In order to derive the effective NHH in the Hubbard model in the context of OQS, we divide the degrees of freedom into a system, describing a single particle, $(\boldsymbol{k_0},\sigma)$, at momentum $\boldsymbol{k_0}$ in spin-state σ, and a bath, which includes the rest of the electrons, see Fig. 1. Thus, the total Hubbard Hamiltonian is divided into the Hamiltonian of the system, $\mathcal{H}_S$, the Hamiltonian of the bath, $\mathcal{H}_B$, and the coupling between system and bath, $\mathcal{H}_c$. The Hamiltonian becomes

$$\mathcal{H}_{\mathrm{tot}} = \sum_{\boldsymbol{k},\sigma}(\epsilon_{\boldsymbol{k}}+\mu_c)c^\dagger_{\boldsymbol{k}\sigma}c_{\boldsymbol{k}\sigma} + U\sum_i n_{i\uparrow}n_{i\downarrow}, \tag{1}$$

$$= \mathcal{H}_S + \mathcal{H}_B + \mathcal{H}_c, \tag{2}$$

$$\mathcal{H}_S = (\epsilon_{\boldsymbol{k_0}}+\mu_c+Un_{\bar\sigma})c^\dagger_{\boldsymbol{k_0}\sigma}c_{\boldsymbol{k_0}\sigma} = \xi c^\dagger_{\boldsymbol{k_0}\sigma}c_{\boldsymbol{k_0}\sigma}, \tag{3}$$

$$\mathcal{H}_B = \sum_{(\boldsymbol{k},\sigma')\neq(\boldsymbol{k_0},\sigma)}(\epsilon_{\boldsymbol{k}}+\mu_c)c^\dagger_{\boldsymbol{k}\sigma'}c_{\boldsymbol{k}\sigma'} + \frac{U}{N}\sum_{\sigma'}\sum_{\substack{\boldsymbol{k_1},\boldsymbol{k_2},\\ \boldsymbol{k_3},\boldsymbol{k_4}\\ \neq(\boldsymbol{k_0},\sigma)}}\delta_{\boldsymbol{k_1}+\boldsymbol{k_3},\boldsymbol{k_2}+\boldsymbol{k_4}}c^\dagger_{\boldsymbol{k_1}\sigma'}c_{\boldsymbol{k_2}\sigma'}c^\dagger_{\boldsymbol{k_3}\bar\sigma'}c_{\boldsymbol{k_4}\sigma'}, \tag{4}$$

$$\mathcal{H}_c = \frac{U}{N}\sum_{\substack{\boldsymbol{k_1},\boldsymbol{k_2},\boldsymbol{k_3}\\ \neq\boldsymbol{k_0}}}\delta_{\boldsymbol{k_1}+\boldsymbol{k_3},\boldsymbol{k_0}+\boldsymbol{k_2}}(c^\dagger_{\boldsymbol{k_0}\sigma}c_{\boldsymbol{k_1}\sigma}c^\dagger_{\boldsymbol{k_2}\bar\sigma}c_{\boldsymbol{k_3}} + \mathrm{H.c.}),$$

$$= \frac{U}{N}(\mathcal{C}^\dagger_\sigma\otimes\mathcal{B}_\sigma + \mathrm{H.c.}), \tag{5}$$

$$\mathcal{C}_\sigma = c_{\boldsymbol{k_0}\sigma}, \tag{6}$$

$$\mathcal{B}_\sigma = \sum_{\substack{\boldsymbol{k_1},\boldsymbol{k_2},\boldsymbol{k_3}\\ \neq\boldsymbol{k_0}}}\delta_{\boldsymbol{k_1}+\boldsymbol{k_3},\boldsymbol{k_0}+\boldsymbol{k_2}}c_{\boldsymbol{k_1}\sigma}c^\dagger_{\boldsymbol{k_2}\bar\sigma}c_{\boldsymbol{k_3}\bar\sigma}, \tag{7}$$

where $c^{(\dagger)}_{\boldsymbol{k}\sigma}$ is an annihilation (creation) operator of an electron in momentum $\boldsymbol{k}$ and spin-direction σ. $\epsilon_{\boldsymbol{k}}$ is the energy dispersion, μ_c is the chemical potential, U is the Hubbard interaction, and N is the number of the lattice sites. Note that the coupling between the system and the bath corresponds to a part of the two-particle interaction.

Starting from the von Neumann equation for the density matrix of the full system, $(d/dt)\rho(t) = -i[H,\rho(t)]$, we derive the QME for the density matrix of the system in second-order perturbation in $\mathcal{H}_c$,

$$\frac{\partial}{\partial t}\rho^I_S(t) = -\int_{t_0}^{t} ds\,\mathrm{tr}_B[\mathcal{H}_c(t),[\mathcal{H}_c(s),\rho^I_S(s)\otimes\rho_B]], \tag{8}$$

where $\rho^I_S(t)$ is the density matrix of the system, i.e., the single particle. We here use the interaction representation $\rho^I(t) = e^{i\mathcal{H}_S t}\rho(t)e^{-i\mathcal{H}_S t}$ and $\mathcal{H}_c(t) = e^{i(\mathcal{H}_S\otimes\mathbf{1}_B+\mathbf{1}_S\otimes\mathcal{H}_B)t}\mathcal{H}_c e^{-i(\mathcal{H}_S\otimes\mathbf{1}_B+\mathbf{1}_S\otimes\mathcal{H}_B)t}$.

The commutators in Eq. (8)) include terms such as [39]

$$\mathcal{C}^\dagger_\sigma\mathcal{C}_\sigma\rho_S(s)\otimes\mathrm{Tr}_B[\mathcal{B}_\sigma(t)\mathcal{B}^\dagger_\sigma(s)\rho_B]$$
$$= \mathcal{C}^\dagger_\sigma\mathcal{C}_\sigma\rho_S(s)\otimes\mathrm{Tr}_B\Bigg[\sum_{\boldsymbol{k_1},\boldsymbol{k_2},\boldsymbol{k_3}}\delta_{\boldsymbol{k_1}+\boldsymbol{k_3},\boldsymbol{k_0}+\boldsymbol{k_2}}$$
$$\times c_{\boldsymbol{k_1}\sigma}(t)c^\dagger_{\boldsymbol{k_2}\bar\sigma}(t)c_{\boldsymbol{k_3}\bar\sigma}(t)c^\dagger_{\boldsymbol{k_3}\bar\sigma}(s)c_{\boldsymbol{k_2}\bar\sigma}(s)c^\dagger_{\boldsymbol{k_1}\sigma}(s)\rho_B\Bigg]. \tag{9}$$

This trace over three creation and three annihilation operators including the time evolution by the full Hamiltonian, only missing the scattering via $(\boldsymbol{k}_0,\ \sigma)$, appears in the second-order diagram for the self-energy shown in Fig. 2.

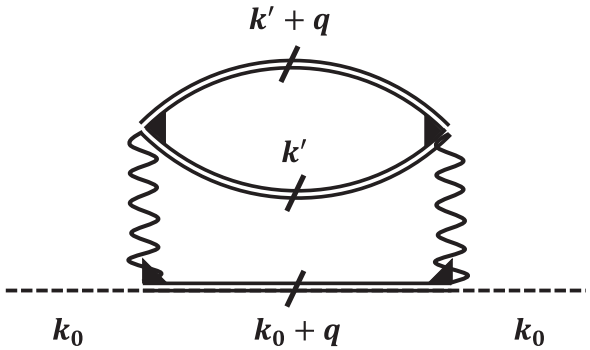

FIG. 2. Feynman diagram which describes the dynamics of the QME in the second order. The slashed double lines correspond to full Green's function which do not include the scattering to $\boldsymbol{k}_0$. The black triangle corresponds to the full two-particle vertex, which does not include scattering via $\boldsymbol{k}_0$.

Because the amplitude of a single scattering process via $\boldsymbol{k}_0$ vanishes in the limit of an infinite large bath, $N \to \infty$, the self-energy shown in Fig. 2 becomes the exact self-energy in second-order perturbation in $\mathcal{H}_c$ (not U). Even when considering higher-order perturbations in $\mathcal{H}_c$, we find that the QME still can be described by the self-energy [39]. Collecting all terms in Eq. (8)), we obtain

$$\begin{aligned}\frac{\partial}{\partial t}\rho_S^I(t) = \int_{t_0}^{t} ds[-i\mathrm{Re}[S_l(t-s)][\mathcal{C}_\sigma^\dagger \mathcal{C}_\sigma, \rho_S^I(s)] \\ + i\mathrm{Re}[S_g(t-s)][\mathcal{C}_\sigma \mathcal{C}_\sigma^\dagger, \rho_S^I(s)] \\ + \mathrm{Im}[S_l(t-s)](\{\mathcal{C}_\sigma^\dagger \mathcal{C}_\sigma, \rho_S^I(s)\} - 2\mathcal{C}_\sigma \rho_S^I(s)\mathcal{C}_\sigma^\dagger) \\ + \mathrm{Im}[S_g(t-s)](\{\mathcal{C}_\sigma \mathcal{C}_\sigma^\dagger, \rho_S^I(s)\} - 2\mathcal{C}_\sigma^\dagger \rho_S^I(s)\mathcal{C}_\sigma)],\end{aligned} \tag{10}$$

with

$$\begin{aligned}S_l(t) &= \Sigma_{\boldsymbol{k}_0}^T(t)e^{i\xi t} \\ S_g(t) &= [\Sigma_{\boldsymbol{k}_0}^R(t) - \Sigma_{\boldsymbol{k}_0}^T(t)]e^{i\xi t}\end{aligned}$$

where Σ^T is the time-ordered self-energy, Σ^R is the retarded self-energy, and $\xi = \epsilon_{\boldsymbol{k}_0} + \mu_c + Un_{\bar{\sigma}}$.

We see that the time evolution of the density matrix of a single particle at $(\boldsymbol{k}_0, \sigma)$ is governed by the self-energy $\Sigma_{\boldsymbol{k}_0}^{R/T}(s)$. However, because Eq. (10)) includes gain and loss terms, i.e., $2\mathcal{C}_\sigma \rho_S^I(s)\mathcal{C}_\sigma^\dagger$ and $2\mathcal{C}_\sigma^\dagger \rho_S^I(s)\mathcal{C}_\sigma$, the dynamics cannot be described by an effective NHH alone.

We next fix the particle number of the system, which corresponds to applying postselection. We restrict the Hilbert space to states where $c_{\boldsymbol{k}_0\sigma}^\dagger c_{\boldsymbol{k}_0\sigma} + c_{\boldsymbol{k}_0\bar{\sigma}}^\dagger c_{\boldsymbol{k}_0\bar{\sigma}} = 1$. We furthermore assume the absence of magnetism, which results in $c_{\boldsymbol{k}_0\sigma}^\dagger c_{\boldsymbol{k}_0\sigma} = c_{\boldsymbol{k}_0\sigma} c_{\boldsymbol{k}_0\sigma}^\dagger$ in the restricted Hilbert space. Due to these restrictions, the gain and loss terms vanish in Eq. (10)), and the commutators and anticommutators can be summed up

$$\begin{aligned}&\frac{\partial}{\partial t}\rho_S^{I\mathrm{PS}}(t) \\ &= -i\int_{t_0}^{t} ds(\mathcal{S}_{\mathrm{eff}}(t-s)\rho_S^{I\mathrm{PS}}(s) - \rho_S^{I\mathrm{PS}}(s)\mathcal{S}_{\mathrm{eff}}^\dagger(t-s))\end{aligned} \tag{11}$$

$$\mathcal{S}_{\mathrm{eff}}(t-s) = \Sigma_{\boldsymbol{k}_0}^R(t-s)e^{i\xi(t-s)}c_{\boldsymbol{k}_0\sigma}^\dagger c_{\boldsymbol{k}_0\sigma}, \tag{12}$$

where $\rho_S^{(I)\,\mathrm{PS}}(t)$ is the density matrix with applied postselection. By using the Markov approximation, which means $\rho_S(s) \to \rho_S(t)$ and $t_0 \to -\infty$, we find that the density matrix of a single particle under postselection can be written as

$$\frac{\partial}{\partial t}\rho_S^{\mathrm{PS}}(t) = -i(\mathcal{H}_{\mathrm{eff}}\rho_S^{\mathrm{PS}}(t) - \rho_S^{\mathrm{PS}}(t)\mathcal{H}_{\mathrm{eff}}^\dagger), \tag{13}$$

$$\mathcal{H}_{\mathrm{eff}} = \mathcal{H}_0 + \Sigma_{\boldsymbol{k}_0}^R(\xi)c_{\boldsymbol{k}_0\sigma}^\dagger c_{\boldsymbol{k}_0\sigma}, \tag{14}$$

which corresponds to the von Neumann equation with an effective NHH. Thus, the time evolution of the density matrix of a single particle $(\boldsymbol{k}_0, \sigma)$ is given by an effective NHH including the self-energy, if postselection is applied [50]. We note that the frequency dependence of the self-energy has vanished because of the Markov approximation.

However, in the context of SCS, the Green's function is described by an effective NHH without postselection [40,42–44,46–48]. To clarify the reason why postselection is not necessary in this context, we will now introduce the retarded Green's function in the steady state using the density matrix form, which is given as $G_{\mathrm{OQS}}^R(t) = -i\Theta(t)\mathrm{Tr}[(\mathcal{C}(t)\mathcal{C}^\dagger(0) + \mathcal{C}^\dagger(0)\mathcal{C}(t))\rho_S^{\mathrm{SS}} \otimes \rho_B]$. Here, ρ_S^{SS} is the density matrix of the system in the long-time limit (steady state) [51] and $\mathcal{C}(t) = e^{i\mathcal{H}_{\mathrm{tot}}t}\mathcal{C}e^{-i\mathcal{H}_{\mathrm{tot}}t}$. Combining the density matrix, ρ_S^{SS}, with the creation operator, $\mathcal{C}^\dagger$, we define the density matrix describing the single-particle Green's function, $\rho_S^{\mathrm{RGF}} = \mathcal{C}^\dagger\rho_S^{\mathrm{SS}} + \rho_S^{\mathrm{SS}}\mathcal{C}^\dagger$. Thus, we can rewrite the Green's function as

$$G_{\mathrm{OQS}}^R(t) = -i\Theta(t)\mathrm{Tr}[\mathcal{C}\rho_S^{\mathrm{RGF}}(t)],$$

where the time evolution of $\rho_S^{\mathrm{RGF}}(t)$ is given by the QME in Eq. (10)).

When considering a system which includes only a single particle, $(\boldsymbol{k}_0, \sigma)$, $\rho_S^{\mathrm{RGF}}(t)$ is given by the following matrix element, $|\sigma\rangle\langle 0|$, where $|\sigma\rangle = c_{\boldsymbol{k}_0,\sigma}^\dagger|0\rangle$. Gain and loss terms vanish in the time evolution for this matrix element, because $\mathcal{C}^\dagger|\sigma\rangle\langle 0|\mathcal{C} = \mathcal{C}|\sigma\rangle\langle 0|\mathcal{C}^\dagger = 0$. Therefore, the QME can be written as

$$\begin{aligned}\frac{\partial}{\partial t}\rho_S^{I\mathrm{RGF}}(t) = -i\int_{t_0}^{t} ds(\mathcal{S}_{\mathrm{eff}}(t-s)\rho_S^{I\mathrm{RGF}}(s) \\ - \rho_S^{I\mathrm{RGF}}(s)\mathcal{S}_{\mathrm{eff}}^\dagger(t-s))\end{aligned} \tag{15}$$

$$\Rightarrow -i\omega\rho_S^{\mathrm{RGF}}(\omega) - \rho_S^{\mathrm{RGF}}(t_0), \tag{16}$$

$$\begin{aligned}&= -i(\mathcal{H}_{\mathrm{eff}}(\omega)\rho_S^{\mathrm{RGF}}(\omega) - \rho_S^{\mathrm{RGF}}(\omega)\mathcal{H}_{\mathrm{eff}}^\dagger(\omega)), \\ &= -i\mathcal{H}_{\mathrm{eff}}(\omega)\rho_S^{\mathrm{RGF}}(\omega),\end{aligned} \tag{17}$$

$$\mathcal{H}_{\mathrm{eff}}(\omega) = \mathcal{H}_0 + \Sigma_{\boldsymbol{k}_0}^R(\omega)c_{\boldsymbol{k}_0,\sigma}^\dagger c_{\boldsymbol{k}_0,\sigma}. \tag{18}$$

The equality in Eq. (17)) holds because ρ_S^{RGF} is proportional to $|\sigma\rangle\langle 0|$ and $\rho_S^{\mathrm{RGF}}\mathcal{H}_{\mathrm{eff}}^\dagger$ becomes zero. Then, the Green's function becomes

$$G_{\mathrm{OQS}}^R(\omega) = -i\mathrm{Tr}[\mathcal{C}\rho_S^{\mathrm{RGF}}(\omega)] = \frac{1}{\omega - \xi - \Sigma_{\boldsymbol{k}_0}^R(\omega)}. \tag{19}$$

We here have demonstrated the following statements: first, the Green's function of a single particle described as

an OQS and its effective NHH is identical to the Green's function and its NHH in closed equilibrium systems. Second, the dynamics of ρ_S^{PS} and ρ_S^{RGF} are described by the same equations, Eqs. (11)) and (15)). We can conclude that the effective NHH describing the dynamics under postselection is identical to the effective NHH describing the Green's function in SCS. Thus, we can analyze non-Hermitian phenomena, which are observable in OQSs under postselection, by studying the spectral function $A(\omega) = -(1/\pi)\mathrm{Im}G^R_{\mathrm{OQS}}(\omega)$ in equilibrium or the nonequilibrium steady state. While postselection becomes increasingly difficult in large systems, the analysis of spectral properties remains feasible. We note that non-Hermitian properties may occur in different response functions than the single-particle spectral function and that the correspondence between the NHH in the density matrix under postselection and the NHH in the response function depends on the kind of the postselection. Third, because the density matrix describing the Green's functions in the context of OQS is given by the off-diagonal matrix element, i.e., $|\uparrow\rangle\langle 0|$, gain and loss terms vanish in the QME, and postselection is unnecessary to derive an effective NHH. We note that, even if we consider larger systems, for example a system including $(\boldsymbol{k_0}, \uparrow)$ and $(\boldsymbol{k_0}, \downarrow)$, gain and loss contributions in the QME for the Green's function vanish [39].

Dynamics of the Hubbard model in the quantum master equation.—Finally, we use the above-introduced QME to describe single-particle properties in the Hubbard model on a 2D square lattice. We furthermore show that the Markov approximation, which ignores the memory effect of the QME dynamics, fails to describe the full spectral function in the Mott phase of the Hubbard model in which non-Markovian dynamics plays an important role.

We have shown above that the time evolution of the density matrix is determined by the self-energy in the QME. We here use the dynamical mean field theory (DMFT) combined with the numerical renormalization group (NRG) to calculate an approximate self-energy [52–54]. Using the self-energy obtained by DMFT combined with NRG in the QME, Eq. (10)), we show the relaxation dynamics of the density matrix into the steady state, and demonstrate that the spectral function calculated by the QME approach is identical with the spectral function directly obtained by DMFT/NRG.

In Fig. 3, we compare the spectral functions calculated by the QME and by DMFT and NRG for the weak-coupling regime [Fig. 3(a)] and the Mott insulator [Fig. 3(c)] for $\boldsymbol{k_0} = (0.4\pi, 0.4\pi)$. We furthermore include a comparison between the QME approach using the Markov approximation and the full dynamics. In the weak-coupling regime, the spectral functions obtained by DMFT and the QME with and without Markov approximation agree with each other. Figure 3(b) shows the time evolution of the diagonal elements of the density matrix with and without Markov approximation in the QME, Eq. (10)). In the weak-coupling regime, memory effects are not important and therefore the Markov approximation works well. The dynamics without memory effects is given by an exponential decay as shown in Fig. 3(b). We conclude that the Markov approximation can describe the full dynamics of the system in the weak-coupling regime, Figs. 3(a) and 3(b).

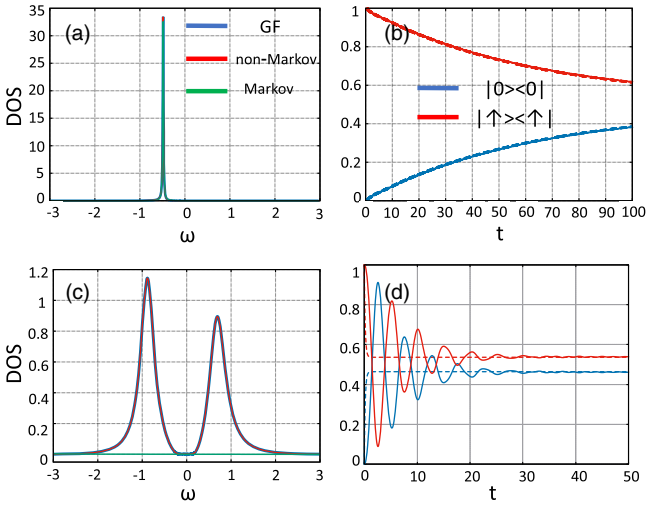

FIG. 3. Spectral function and the time evolution of the diagonal elements into the steady state in the weak-coupling regime and in the Mott insulating phase. The parameters in panels (a) and (b) are as follows: $\epsilon_k = -0.49, \mu_c = -0.2$, $U = 0.4$, and the temperature $T = 0.001$. The parameters in panels (c) and (d) are as follows: $\epsilon_k = -0.12$, $t = 0.1$, $\mu_c = -0.8$, $U = 1.6, T = 0.00006$. The blue, red, and green lines in (a) and (c) show the spectral function as calculated by the Green's function, non-Markov QME [Eq. (15))], and the Markov QME [Eq. (13))], respectively. The blue and the red lines in (b) and (d) show the dynamics of the diagonal elements $|0\rangle\langle 0|$ and $|\uparrow\rangle\langle\uparrow|$ from the initial state $\rho_i = |\uparrow\rangle\langle\uparrow|$. The full lines and the dashed lines correspond to the non-Markovian dynamics and the Markovian dynamics, respectively.

In the Mott-insulating phase, shown in Fig. 3(c), the non-Markov spectral function does also agree with the spectral function obtained by DMFT and NRG. On the other hand, the spectral function calculated with the Markov approximation is nearly zero. In the Mott insulating regime, the Markov approximation describes strong dissipation due to the strong scattering with the bath electrons and the resulting spectral function has only a small and wide peak. We note, however, that the integral of over the frequency is unity. Non-Markovian dynamics is essential to correctly describe the strongly interacting system. Both peaks in the spectral function are described by quasiparticles which follow non-Markovian dynamics. In Fig. 3(d), we show the dynamics of the diagonal elements of the density matrix comparing between Markovian and non-Markovian dynamics. Both approaches show a strong decay into the same steady state. Additional to the strong decay of the matrix element of the density matrix, the non-Markovian

dynamics show a strong oscillatory behavior of the occupation number.

In the Supplemental Material [39], we perform a similar analysis for the periodic Anderson model, showing that also in this model the spectral function of a small system described as an OQS and its effective NHH are identical to the Green's function and its NHH in closed equilibrium systems.

Summary and discussion.—By analyzing the Hubbard model as an OQS, we have proved that the effective NHH appearing in the context of OQS and equilibrium Green's functions are identical. We have demonstrated that the spectral function of a single particle described as an OQS is given by the same non-Hermitian Hamiltonian describing the density matrix of the particle under postselection. Thus, non-Hermitian phenomena that have been analyzed in the dynamics of a system under postselection can also be studied by analyzing spectral functions both in OQS and SCS without postselection. We have also shown that postselection is not necessary to derive a NHH from the spectral function, because off-diagonal elements govern the dynamics of the spectral function, and gain and loss contributions automatically vanish. In the process of deriving the QME for a single particle, we have succeeded in showing that Feynman diagrams, e.g., representing the self-energy, describe the non-Markovian dynamics of a fermionic system coupled to a fermionic bath. This technique might also be applied to other systems, such as QuBits coupled to fermionic baths. Finally, we have demonstrated the importance of non-Markovian dynamics to describe the dynamics in the strongly correlated regime.

Y. M. thanks C. Uchiyama, I. Hashimoto, K. Mizuta, K. Takasan, N. Hatano, and T. Mori for fruitful discussion and valuable comments. This work is partly supported by JSPS KAKENHI Grants No. JP18H04316 and No. JP18K03511. Computer simulations were performed on the supercomputer of the ISSP in the University of Tokyo.

*michishita.yoshihiro.56e@st.kyoto-u.ac.jp
†peters@scphys.kyoto-u.ac.jp

[1] H. Shen, B. Zhen, and L. Fu, Phys. Rev. Lett. **120**, 146402 (2018).
[2] N. Hatano and D. R. Nelson, Phys. Rev. B **56**, 8651 (1997).
[3] M. Liertzer, L. Ge, A. Cerjan, A. D. Stone, H. E. Türeci, and S. Rotter, Phys. Rev. Lett. **108**, 173901 (2012).
[4] M. Brandstetter, M. Liertzer, C. Deutsch, P. Klang, J. Schöberl, H. Türeci, G. Strasser, K. Unterrainer, and S. Rotter, Nat. Commun. **5**, 4034 (2014).
[5] P. San-Jose, J. Cayao, E. Prada, and R. Aguado, Sci. Rep. **6**, 21427 (2016).
[6] J. Doppler, A. A. Mailybaev, J. Böhm, U. Kuhl, A. Girschik, F. Libisch, T. J. Milburn, P. Rabl, N. Moiseyev, and S. Rotter, Nature (London) **537**, 76 (2016).
[7] T. E. Lee, Phys. Rev. Lett. **116**, 133903 (2016).
[8] Y. Ashida, S. Furukawa, and M. Ueda, Nat. Commun. **8**, 15791 (2017).
[9] W. Chen, Ş. K. Özdemir, G. Zhao, J. Wiersig, and L. Yang, Nature (London) **548**, 192 (2017).
[10] L. Feng, R. El-Ganainy, and L. Ge, Nat. Photonics **11**, 752 (2017).
[11] Z. Gong, Y. Ashida, K. Kawabata, K. Takasan, S. Higashikawa, and M. Ueda, Phys. Rev. X **8**, 031079 (2018).
[12] M. Nakagawa, N. Kawakami, and M. Ueda, Phys. Rev. Lett. **121**, 203001 (2018).
[13] F. K. Kunst, E. Edvardsson, J. C. Budich, and E. J. Bergholtz, Phys. Rev. Lett. **121**, 026808 (2018).
[14] S. Yao and Z. Wang, Phys. Rev. Lett. **121**, 086803 (2018).
[15] S. Yao, F. Song, and Z. Wang, Phys. Rev. Lett. **121**, 136802 (2018).
[16] K. Kawabata, K. Shiozaki, M. Ueda, and M. Sato, Phys. Rev. X **9**, 041015 (2019).
[17] K. Kawabata, S. Higashikawa, Z. Gong, Y. Ashida, and M. Ueda, Nat. Commun. **10**, 297 (2019).
[18] T. Helbig, T. Hofmann, S. Imhof, M. Abdelghany, T. Kiessling, L. W. Molenkamp, C. H. Lee, A. Szameit, M. Greiter, and R. Thomale, arXiv:1907.11562.
[19] A. Ghatak, M. Brandenbourger, J. van Wezel, and C. Coulais, arXiv:1907.11619.
[20] L. Xiao, T. Deng, K. Wang, G. Zhu, Z. Wang, W. Yi, and P. Xue, Nat. Phys., 1 (2020).
[21] T. Hofmann, T. Helbig, F. Schindler, N. Salgo, M. Brzeziska, M. Greiter, T. Kiessling, D. Wolf, A. Vollhardt, A. Kabai, C. H. Lee, A. Bilui, R. Thomale, and T. Neupert, arXiv:1908.02759.
[22] N. Okuma, K. Kawabata, K. Shiozaki, and M. Sato, Phys. Rev. Lett. **124**, 086801 (2020).
[23] C. H. Lee and R. Thomale, Phys. Rev. B **99**, 201103(R) (2019).
[24] D. S. Borgnia, A. J. Kruchkov, and R.-J. Slager, Phys. Rev. Lett. **124**, 056802 (2020).
[25] K. Yamamoto, M. Nakagawa, K. Adachi, K. Takasan, M. Ueda, and N. Kawakami, Phys. Rev. Lett. **123**, 123601 (2019).
[26] Z. Lin, H. Ramezani, T. Eichelkraut, T. Kottos, H. Cao, and D. N. Christodoulides, Phys. Rev. Lett. **106**, 213901 (2011).
[27] A. Regensburger, C. Bersch, M.-A. Miri, G. Onishchukov, D. N. Christodoulides, and U. Peschel, Nature (London) **488**, 167 (2012).
[28] L. Feng, Z. J. Wong, R.-M. Ma, Y. Wang, and X. Zhang, Science **346**, 972 (2014).
[29] C. Dembowski, H.-D. Gräf, H. L. Harney, A. Heine, W. D. Heiss, H. Rehfeld, and A. Richter, Phys. Rev. Lett. **86**, 787 (2001).
[30] B. Peng, Ş. K. Özdemir, F. Lei, F. Monifi, M. Gianfreda, G. L. Long, S. Fan, F. Nori, C. M. Bender, and L. Yang, Nat. Phys. **10**, 394 (2014).
[31] T. Gao, E. Estrecho, K. Bliokh, T. Liew, M. Fraser, S. Brodbeck, M. Kamp, C. Schneider, S. Höfling, Y. Yamamoto *et al.*, Nature (London) **526**, 554 (2015).
[32] H. Xu, D. Mason, L. Jiang, and J. Harris, Nature (London) **537**, 80 (2016).
[33] T. E. Lee and C.-K. Chan, Phys. Rev. X **4**, 041001 (2014).
[34] J. Wiersig, Phys. Rev. Lett. **112**, 203901 (2014).

[35] Z.-P. Liu, J. Zhang, S. K. Özdemir, B. Peng, H. Jing, X.-Y. Lü, C.-W. Li, L. Yang, F. Nori, and Y.-x. Liu, Phys. Rev. Lett. **117**, 110802 (2016).
[36] H. Hodaei, A. U. Hassan, S. Wittek, H. Garcia-Gracia, R. El-Ganainy, D. N. Christodoulides, and M. Khajavikhan, Nature (London) **548**, 187 (2017).
[37] J. W. Yoon, Y. Choi, C. Hahn, G. Kim, S. H. Song, K.-Y. Yang, J. Y. Lee, Y. Kim, C. S. Lee, J. K. Shin *et al.*, Nature (London) **562**, 86 (2018).
[38] H.-K. Lau and A. A. Clerk, Nat. Commun. **9**, 4320 (2018).
[39] See the Supplemental Material at http://link.aps.org/supplemental/10.1103/PhysRevLett.124.196401 for (i) a brief explanation about the postselection, (ii) a detailed explanation for the reason why the quantum master equation can be described by the self-energy, (iii) proof that the gain and loss contribution to the Green's function disappears in general open quantum systems, and (iv) correspondence of the effective non-Hermitian Hamiltonians in the context of open quantum systems and strongly correlated systems in the periodic Anderson model, which includes Refs. [40,41].
[40] Y. Michishita, T. Yoshida, and R. Peters, Phys. Rev. B **101**, 085122 (2020).
[41] H.-P. Breuer, F. Petruccione *et al.*, *The Theory of Open Quantum Systems* (Oxford University Press on Demand, New York, 2002).
[42] V. Kozii and L. Fu, arXiv:1708.05841.
[43] T. Yoshida, R. Peters, and N. Kawakami, Phys. Rev. B **98**, 035141 (2018).
[44] T. Yoshida, R. Peters, N. Kawakami, and Y. Hatsugai, Phys. Rev. B **99**, 121101(R) (2019).
[45] N. C. Chávez, F. Mattiotti, J. A. Méndez-Bermúdez, F. Borgonovi, and G. Luca Celardo, Eur. Phys. J. B **92**, 144 (2019).
[46] P. A. McClarty and J. G. Rau, Phys. Rev. B **100**, 100405(R) (2019).
[47] K. Kimura, T. Yoshida, and N. Kawakami, Phys. Rev. B **100**, 115124 (2019).
[48] T. Matsushita, Y. Nagai, and S. Fujimoto, Phys. Rev. B **100**, 245205 (2019).
[49] H. Shen and L. Fu, Phys. Rev. Lett. **121**, 026403 (2018).
[50] We have shown here that the dynamics of the single-particle Hilbert space is determined by the self-energy of the single-particle in the total system. The imaginary part of the effective Hamiltonian (corresponding to the imaginary part of the self-energy) is equivalent to the sum of the gain and loss terms, and it causes a decay of the norm of the density matrix, ρ_S^{PS}. This decay of the norm means that the possibility of obtaining results, in which gain or loss (electron-electron scattering) does not occur and the particle number does not change, decreases in time. Therefore, the imaginary part of the self-energy can be interpreted as the inverse of the lifetime of the quasiparticle, as it is well known in the context of the strongly correlated electron systems. On the other hand, the real part of the self-energy describes the correction of the energy levels due to the coupling with the bath. Thus, these kinds of two-particle interaction effects are included in the dynamics of the single-particle Hilbert space and the dynamics is determined by the self-energy.
[51] Because the total system is isolated, we here suppose that it reaches the equilibrium (steady-state) state. Therefore, if we consider the exact non-Markovian dynamics, the density matrix of the system is given as $\rho_S^{\mathrm{SS}} = \mathcal{P}\rho_{\mathrm{total}}^{\mathrm{eq}}\mathcal{P}$, where $\mathcal{P}$ is the projection operator on the Hilbert space of the system and $\rho_{\mathrm{total}}^{\mathrm{eq}}$ is the density matrix of the equilibrium state of the total system.
[52] A. Georges, G. Kotliar, W. Krauth, and M. J. Rozenberg, Rev. Mod. Phys. **68**, 13 (1996).
[53] R. Bulla, T. A. Costi, and T. Pruschke, Rev. Mod. Phys. **80**, 395 (2008).
[54] R. Peters, T. Pruschke, and F. B. Anders, Phys. Rev. B **74**, 245114 (2006).